Molecular Crystals and Liquid Crystals Science and Technology. Section A. Molecular Crystals and Liquid Crystals
Publication details, including instructions for authors and subscription information:
http://www.tandfonline.com/loi/gmcl19

Time-Resolved FT-IR Analysis of Electric Field-Induced Reorientation Dynamics in Nematic 4-Pentyl-(4-cyanophenyl)-Cyclohexane Liquid Crystals

H. Sugisawa [a b], H. Toriumi [a] & H. Watanabe [a]
[a] Department of Chemistry, College of Arts and Sciences, University of Tokyo, Komaba, Meguro, Tokyo, 153, Japan
[b] Japan Electron Optics Laboratory Ltd. (JEOL), Akishima, Tokyo, 196, Japan
Version of record first published: 24 Sep 2006.

To cite this article: H. Sugisawa , H. Toriumi & H. Watanabe (1992): Time-Resolved FT-IR Analysis of Electric Field-Induced Reorientation Dynamics in Nematic 4-Pentyl-(4-cyanophenyl)-Cyclohexane Liquid Crystals, Molecular Crystals and Liquid Crystals Science and Technology. Section A. Molecular Crystals and Liquid Crystals, 214:1, 11-22

To link to this article: http://dx.doi.org/10.1080/10587259208037278

Mol. Cryst. Liq. Cryst., 1992, Vol. 214, pp. 11–22
Reprints available directly from the publisher
Photocopying permitted by license only

Printed in the United States of America

Time-Resolved FT-IR Analysis of Electric Field-Induced Reorientation Dynamics in Nematic 4-Pentyl-(4-cyanophenyl)-cyclohexane Liquid Crystals

H. SUGISAWA,† H. TORIUMI‡ and H. WATANABE

Department of Chemistry, College of Arts and Sciences, University of Tokyo, Komaba, Meguro, Tokyo 153, Japan

(Received August 27, 1991; in final form October 17, 1991)

The application of rapid-scan FT-IR time-resolved spectroscopy to the study of molecular reorientation dynamics in a nematic liquid crystal during the electric field-induced homogeneous-to-homeotropic transition is reported. The average orientation of bond segments in a homogeneously oriented 4-pentyl-(4-cyanophenyl)-cyclohexane liquid crystal is determined from static infrared dichroism measurements. The observed temperature dependence of the molecular orientational order parameter agrees with the prediction of the Maier-Saupe theory. Analysis of time-resolved dichroic spectra shows that the homogeneous-to-homeotropic transition requires an induction period of several milliseconds and is completed in 10–20 ms. The cyanophenyl group reorients as a unit in response to the applied electric field and the reorientation rate increases as temperature is increased.

Keywords: time-resolved FT-IR, nematic 5PCH, homogeneous-homeotropic transition, reorientation dynamics, electro-optic effect

1. INTRODUCTION

There has been wide-spread use of liquid crystals in display devices as they can be readily oriented by applying an external electric field and exhibit various electro-optic effects. Thus, the development of advanced display systems and the search for required new materials have constituted a major part of liquid crystal research in the past two decades. Despite this excitement about new applications, our understanding of the elementary molecular mechanism of the electric field-induced transition in liquid crystals is still limited. In particular, the local conformation and the orientation dynamics of rigid segments constituting a flexible liquid crystalline molecule is not yet clearly elucidated. Acquisition of such knowledge is of fundamental importance toward further progress in both the science and the technology

†Present Address: Japan Electron Optics Laboratory Ltd. (JEOL), Akishima, Tokyo 196, Japan.
‡Author to whom correspondence should be addressed.

of liquid crystals, and this necessitates a new experimental technique that enables us to interrogate about the details of field-induced phenomena of liquid crystals at the molecular segmental level.

In a previous paper[1] we reported the application of rapid-scan FT-IR time-resolved spectroscopy (FT-IR TRS) to the study of the kinetics of electric field-induced reorientation of the nematic 4-pentyl-4′-cyanobiphenyl (5CB) liquid crystal. The applicability of FT-IR TRS was further corroborated in a subsequent study[2] where we employed step-scan two-dimensional FT-IR TRS to analyze the orientational correlation between different segments in the molecule. These studies demonstrate that FT-IR TRS can provide a rich amount of information about both average orientation and its time evolution for liquid crystal molecules under the influence of an external electric field. The most obvious advantage of FT-IR TRS is its capability to obtain temporal and spectral information simultaneously for all IR active absorption bands. This capability is accomplished by taking the inherit advantages of FT-IR spectrometry, namely, the multiplex advantage and the throughput advantage, which provide high efficiency in acquisition of time-resolved infrared interferogram elements. In this paper we describe the fundamentals of the FT-IR TRS experiment using a rapid-scan FT-IR spectrometer and report the results of static and dynamic polarized infrared measurements for the nematic 4-pentyl-(4-cyanophenyl)-cyclohexane (5PCH) liquid crystal during its electric field-induced homogeneous-to-homeotropic transition.

2. FT-IR TIME-RESOLVED SPECTROSCOPY

FT-IR spectrometry, having much higher sensitivity than conventional dispersion IR spectrometry, is capable of performing fast and accurate infrared measurements over a wide range of wavenumbers. Moreover, the introduction of computer-aided data processing systems adds capability to edit a large number of data elements flexibly and quickly. Consideration of these characteristic advantages of modern FT-IR spectrometry leads to the comprehension that this technique can be applied to the analysis of fast electric field-induced transition phenomena exhibited by liquid crystals. The method, which we will describe below, to obtain transient FT-IR spectra is called FT-IR TRS.

In conventional static FT-IR experiments using a rapid-scan spectrometer, spectra are obtained from Fourier transformation of interferograms measured by scanning the moving mirror at a constant speed. Hence, if the sample condition remains unchanged during a time period of mirror scanning, the interferogram is obtained as a simple function of the optical path difference, independent of the mirror scanning speed. However, when the state of the sample evolves on a time scale comparable to the mirror scanning time or even at higher rates, the interferogram will contain two different kinds of information: one is the change in the optical path difference and the other is the variation of interferogram elements reflecting the temporal evolution of the signal from the sample. Hence, in order to obtain time-resolved FT-IR spectra from transient sources, it is necessary to separate the above two time-dependent responses and extract a set of interferograms corresponding to a specific temporal state of the sample.

Figure 1 shows the sampling sequence of time-resolved interferograms in a rapid-scan FT-IR TRS experiment using a JEOL JIR-40X spectrometer. The optical system of this spectrometer consists of the primary Michelson interferometer for the infrared radiation and the two sub-interferometers for the white light and the He-Ne laser beam. The white light interferogram gives a sharp burst and determines the start point of the data acquisition sequence in each moving mirror scan. The monochromatic light interferogram of the He-Ne laser beam gives a sine wave signal and supplies a precise internal time clock for data acquisition and mirror position monitoring. In the first scan of the moving mirror, the spectrometer initiates the whole data acquisition process when it receives a signal from the white light interferometer (indicated by a bold arrow). Then, when the moving mirror reaches the minimum path difference position, the spectrometer samples the first data point ($i = 1$) and, after a certain delay time τ, sends out a signal to an external system that initiates the time dependent phenomenon of the sample. In the present experiment, the signal initiates an electric pulse generator which applies a DC field to the liquid crystal sample (the triggering position is indicated by black arrows). After the time dependent field-induced reorientation of the liquid crystal sample is triggered, acquisition of subsequent data points ($i = 2, 3, \ldots, N$) follows at each discrete time interval (Δt) synchronized by the pulse signals sent from the laser interferometer. In the succeeding scans of the moving mirror, a delay of Δt is added each time before data acquisition and electric-field triggering are started. Note that this time delay Δt is equal to the time interval of data acquisition in each individual sampling sequence. Hence, as seen in Figure 1, the first data points of the time-resolved interferograms are accumulated in the first scan, the second data points in the second scan and so on, with increasing the optical path difference stepwise each time. This process is repeated until the moving mirror arrives at the

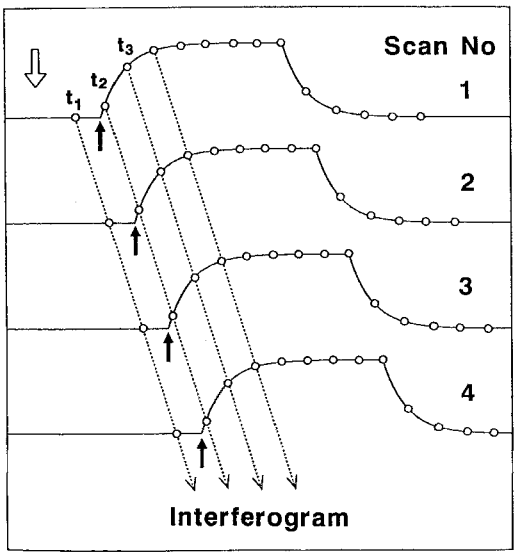

FIGURE 1 Sampling scheme of constant-in-time interferograms in time-resolved rapid-scan FT-IR experiment.

maximum path difference position required for a specified wavenumber resolution. After the whole sampling process is completed, all data are sorted along the dashed lines in Figure 1. The end result of this sorting is a series of interferograms at t_1, t_2, . . . , t_N. Finally, these interferograms are Fourier transformed to give time-resolved FT-IR spectra. Here, the maximum number of time-resolved spectra measured in a single TRS experiment is 40. The only requirement for the sample is that an identical time-dependent phenomenon is repetitive and reproducible for a sufficiently large number of times to complete the whole data set.

The sampling time interval Δt is determined by the modulation frequency of the laser interferogram $f = 2v/\lambda$, where $\lambda = 632.8$ nm is the wavelength of the He-Ne laser light and v is the velocity of the moving mirror. In our JIR-40X spectrometer, v is set at 1.58 mm/s. This gives a modulation frequency of $f = 5$ kHz, which corresponds to a time resolution of $\Delta t = 1/f = 200$ μs (the value of Δt may be alternatively set at 400, 800 and 1600 μs). Measurements at higher time resolution (up to 10 μs) can be made by repeating the same TRS experiment described above and varying the delay time τ stepwise. However, such high time resolution was not necessary to analyze the field-induced reorientation dynamics of the nematic sample examined here.

The FT-IR TRS technique was first developed by Murphy and Sakai[3,4] for step-scan spectrometry, and then applied to rapid-scan FT-IR spectrometry by Mantz.[5] A general description of earlier FT-IR TRS experiments using rapid-scan, step-scan and other techniques can be found in the literature.[6,7]

3. EXPERIMENTAL

All TRS measurements were made at 8 cm^{-1} wavenumber resolution using a JEOL JIR-40X spectrometer. Static dichroic spectra were measured at 2 cm^{-1} resolution for more accurate determination of peak positions and absorbance. The sample of 5PCH, with a nematic temperature range of 30–55°C, was purchased from Merck Japan. The structure of 5PCH is shown in the insert of Figure 4. A variable-temperature liquid-crystal cell was designed to cover a range from room temperature up to 180°C. The structure of this cell is illustrated in Figure 2. The two germanium plates, separated by polyester spacers, served both as windows and as electrodes. These germanium windows were held by aluminum plates through which the windows were electrically connected to an external DC pulse generator. The aluminum plates served also as the thermal conductor with surrounding electric heaters. The cell temperature was monitored by a Pt 100Ω electric resistance thermometer and controlled by a P.I.D. temperature controller to within ±0.1°C.

The inner surfaces of the germanium windows were coated with polyvinylalcohol and rubbed in one direction. The cell was then assembled with the rubbing directions of the two windows parallel to each other. The cell thickness was adjusted by polyester spacers and calculated from the interference pattern of the empty cell. The actual value of thickness was found to be 8.5 μm. The 5PCH sample was injected into this cell, which was preheated above the nematic-isotropic transition temperature of 5PCH, through a gap between the windows along the rubbing

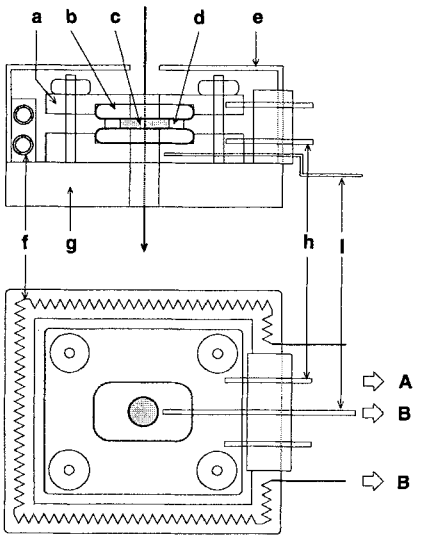

FIGURE 2 Composition of variable-temperature liquid-crystal cell: a; aluminum plate, b; germanium window, c; liquid crystal, d; polyester spacer, e; hood, f; electric heater, g; base, h; copper lead, i; Pt electric resistance thermometer, A; DC pulser, and B; temperature controller.

direction. Then, the cell was transferred to the sample compartment of the spectrometer and cooled slowly into the nematic range so that the molecules align predominantly parallel to the rubbing direction (the homogeneous orientation; Figure 3a). When a sufficiently high electric field is applied normal through the germanium windows, the 5PCH molecules undergo a transition to the homeotropic orientation in which the molecules are oriented parallel to the field direction (Figure 3b). For the dichroism measurements, a rotatable KRS-5 polarizer was placed after the cell.

4. RESULTS AND DISCUSSION

a. Static Dichroism Measurements

Figure 4 shows the polarized infrared absorption spectra of the homogeneously oriented 5PCH liquid crystal sample, measured with the polarizer parallel ($A_{\parallel}$) and perpendicular ($A_{\perp}$) to the rubbing direction. The assignments of major absorption bands, their peak wavenumbers and the values of dichroic ratio D are listed in Table I. The C≡N stretching band at 2226 cm^{-1} and the two phenyl C—C stretching bands at 1607 and 1503 cm^{-1}, all polarized along the *para*-axis of the cyanophenyl group, show large dichroism with D = 3.98, 4.57 and 4.40, respectively. This result confirms that the *para*-axis of the cyanophenyl group is indeed oriented predominantly parallel to the rubbing direction (Figure 3a). The band at 833 cm^{-1} appears as an isolated single peak and has the lowest dichroic ratio D = 0.33. The main contribution to this band comes from the phenyl ring C—H wagging band which is polarized normal to the ring plane. However, a comparison with the

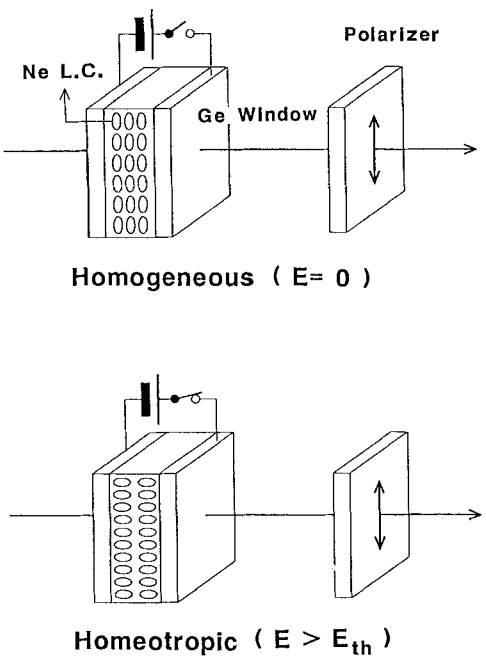

FIGURE 3 Schematic drawings of homogeneous (top) and homeotropic (bottom) liquid crystal orientations.

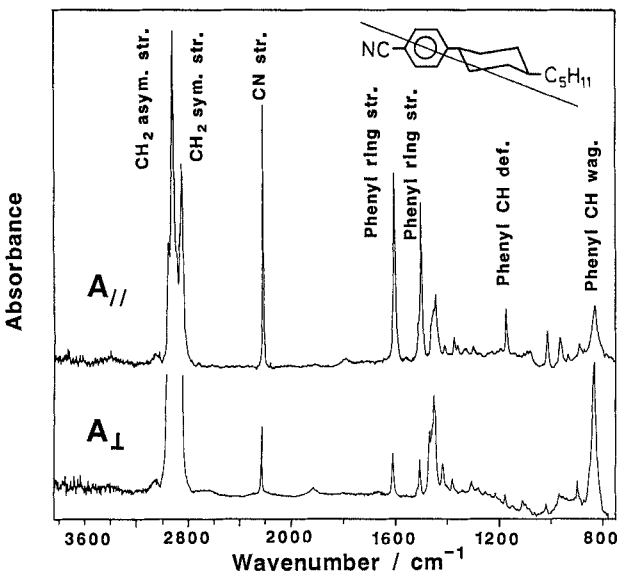

FIGURE 4 Polarized infrared absorption spectra of homogeneously oriented 5PCH liquid crystal at 32°C (wavenumber resolution 2 cm^{-1} and sample thickness 8.5 μm) and the structure of 5PCH.

TABLE I

Infrared polarized absorption data for a homogeneously oriented 5PCH liquid crystal at 32°C (D: dichroic ratio, S_b: degree of orientational order of the transition moment and β: the angle (in degree) of the transition moment relative to the long molecular axis Z

Wavenumber	Assignment	D	S_b	β
2924	CH_2 asym. stretching[a,b]			
2851	CH_2 sym. stretching[a,b]			
2226	C≡N stretching	3.98	0.498	17.5
1607	Phenyl C—C stretching	4.57	0.543	11.3
1503	Phenyl C—C stretching	4.40	0.531	13.2
1447	CH_2 deformation[b,c]	0.65	−0.132	64.9
1177	Phenyl C—H in-plane deformation	4.05	0.504	16.8
833	Phenyl C—H wagging	0.33	−0.288	90.0[d]

[a]Accurate estimation of D is precluded because of high absorbance.
[b]All CH_2 associated bands may include contributions from both cyclohexane ring and pentyl terminal chain.
[c]This band is superimposed on by neighboring absorption bands: The numbers reported are therefore only tentative.
[d]Assumed.

spectrum of 5CB measured in earlier studies[1,8,9] indicates that this peak may be superimposed with the pentyl chain deformation band, which is also polarized in the transverse direction of the long molecular axis. For simplicity, this 833 cm^{-1} band will be called the phenyl C—H wagging band in the following discussion.

The degree of orientational order of the transition moment or, of the bond carrying the transition moment, S_b, is defined as

$$\begin{aligned} S_b &= P_2(\cos\beta)\,\langle P_2(\cos\theta)\rangle \\ &= \tfrac{1}{2}(3\cos^2\beta - 1)\,\langle \tfrac{1}{2}(3\cos^2\theta - 1)\rangle \end{aligned} \tag{1}$$

where β is the orientation angle of the transition moment relative to the long axis of the molecule and θ is the angle between this long axis and the nematic director. To derive Equation 1 we have introduced the usual assumption that the molecules can rotate freely around the long axis and the nematic phase possesses the cylindrical symmetry. The experimental S_b value can be calculated from the dichroic ratio D of the respective absorption band as

$$S_b = (D - 1)/(D + 2) \tag{2}$$

In Figure 5 we plot the S_b values of the three representative absorption bands of 5PCH against temperature. The C≡N stretching band and the phenyl ring C—C stretching band have positive S_b values, while the phenyl C—H wagging band has a negative value with absolute magnitude of approximately one-half of the previous two. All these S_b values decrease with increasing temperature and fall to zero discontinuously at the nematic-isotropic transition temperature T_{NI} = 329K. It may be noticed that S_b of the C≡N stretching band is slightly smaller than that of the phenyl C—C band, indicating the presence of small amplitude thermal fluctuations of the C≡N band.

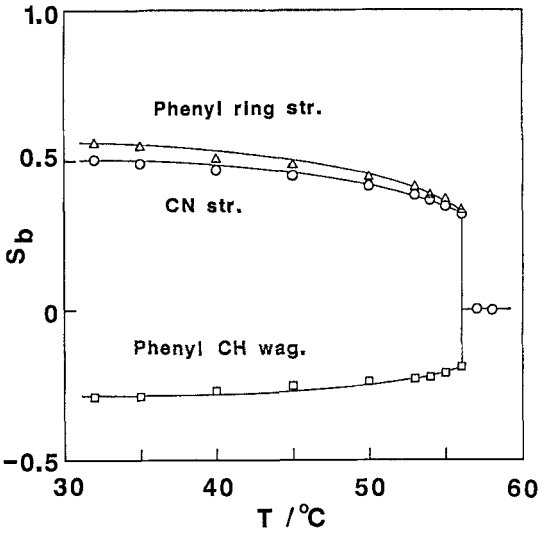

FIGURE 5 Temperature dependence of the bond orientational order parameters S_b calculated for the three absorption bands (the phenyl ring stretching band refers to the one at 1607 cm^{-1}).

The long molecular axis Z, that describes the orientation of the whole molecule, is in a plane formed by the symmetry axes of the phenyl ring and the cyclohexane ring (see the 5PCH structure in Figure 4). Once the angle of orientation (β) of any particular transition moment relative to the Z-axis is determined, we can then calculate the molecular orientational order parameter S which is defined as

$$S = \langle P_2(\cos\theta)\rangle = \langle \tfrac{1}{2}(3\cos^2\theta - 1)\rangle \tag{3}$$

As described above, the transition moment of the phenyl C—H wagging band at 833 cm^{-1} is polarized perpendicular to the phenyl-ring plane, hence it is also perpendicular to the long molecular axis Z. By introducing $\beta = 90°$ we obtain from Equation 1 a simple relation $S = -2S_b$ for this 833 cm^{-1} band. In Figure 6, the experimental S value (open circle) calculated from S_b in Figure 5 is plotted against the reduced temperature (T/T_{NI}). For comparison, a theoretical curve predicted from the Maier-Saupe theory[10] is also shown (solid line). The agreement between experiment and theory is satisfactory. This supports the assumption $\beta = 90°$ made for the 833 cm^{-1} band. A slight, systematic deviation between experiment and theory may arise from the well-known deficiency in the Maier-Saupe theory (such as those associated with the rigid-rod approximation and the mean-field approximation) or from experimental error such as imperfections in homogeneous orientation and ignoring the contributions of the pentyl chain vibrations to the 833 cm^{-1} absorption. Though it is not our major concern to discuss the details of theoretical modeling of liquid crystal orientation, it may be noted that the inclusion of the molecular flexibility and consequent shape anisotropy (both being ignored in the Maier-Saupe theory) have been shown to improve the quantitative description of the orientational order profile of nematic liquid crystals significantly.[11] A more

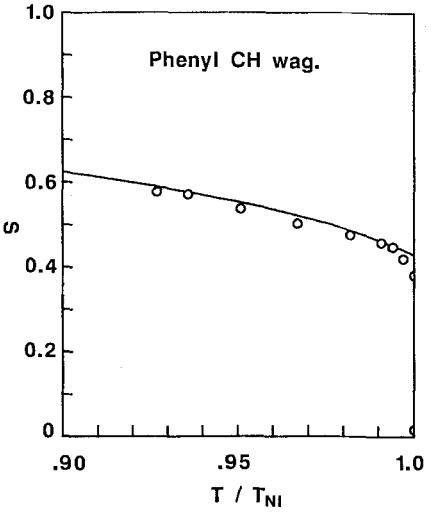

FIGURE 6 Plot of the molecular orientational order parameter S against the reduced temperature T/T_{NI}. Open circles represent the experimental values calculated from the dichroic ratio of the phenyl C—H wagging band and the solid line represents the prediction of the Maier-Saupe theory.

distinct deviation near T_{NI}, where the experimental S value falls more rapidly, should be attributed to inhomogeneous temperature distribution in the sample (near the phase transition point even a very small temperature fluctuation can cause partial melting of the sample).

With the molecular orientational order parameter S determined in Figure 6, we are now able to calculate the orientation angle β of the transition moment relative to the long molecular axis for the remainder of the absorption bands. For example, the angle between the phenyl *para*-axis and the Z-axis is calculated to be $\beta = 11.3-13.2°$ from the D values of the phenyl C—C stretching bands at 1607 and 1503 cm^{-1}. This value is essentially independent of temperature and indicates that the Z-axis orients roughly in a direction connecting the phenyl ring and the cyclohexane ring. The corresponding values calculated for the C≡N stretching band and for the phenyl C—H in-plane deformation band are slightly larger: It should be recognized that their D values are reduced to a certain extent because of thermal fluctuations of the bond. A summary of the values of S_b and β is given in the last two columns of Table I.

b. Time Resolved Measurements

The homogeneously oriented 5PCH liquid crystal undergoes the transition to the homeotropic structure when a sufficiently high electric field is applied (Figure 3b). Dichroic spectra measured as a function of the field strength E show that the homogeneous-to-homeotropic transition takes place above a certain threshold field strength E_{th}. The E_{th} value is about 1.5 V for a 8.5 μm sample and slightly temperature dependent. It is also found that the spectral change due to field application appears only in the parallel absorption spectrum $A_{\parallel}$, while the perpendicular absorption spectrum $A_{\perp}$ does not show any significant changes in the entire E range.

For example, the integrated peak intensities of the C≡N and the phenyl C—C stretching bands in $A_{\parallel}$ undergo a sharp decrease above E_{th} and then gradually approach their equilibrium values. On the other hand, the corresponding values in $A_{\perp}$ remain essentially unchanged. Hence, at sufficiently high fields $A_{\parallel}$ asymptotically approaches $A_{\perp}$. This observation indicates that the reorientation of 5PCH proceeds predominantly in a plane defined by the initial molecular orientation and the direction of the applied electric field. In other words, the homogeneous-to-homeotropic transition of 5PCH can be represented by a 90° rotation of the nematic director. The same result has been reported for 5CB previously.[1,2]

It is clear from the above observation that the information necessary to analyze the dynamics of the homogeneous-to-homeotropic transition can be obtained from time-resolved measurements of parallel polarized absorption spectrum $A_{\parallel}$. Summarized in Figure 7 is the temporal variation of the three representative absorption bands of 5PCH taken from the time-resolved $A_{\parallel}$ spectra. Some details of this experiment are as follows: the temporal resolution is 1.6 ms; the DC pulse field of 5 V, which is several times hgher than E_{th}, is applied at the position indicated by an arrow; and the interferogram is accumulated only once. Although the interferogram is not averaged, the signal-to-noise ratio of the resultant spectrum is satisfactory. As clearly seen in Figure 7, the transition requires an induction period before actual changes in molecular orientation take place. The induction time is approximately 8 ms and the transition is completed in 10–20 ms. The peak in-

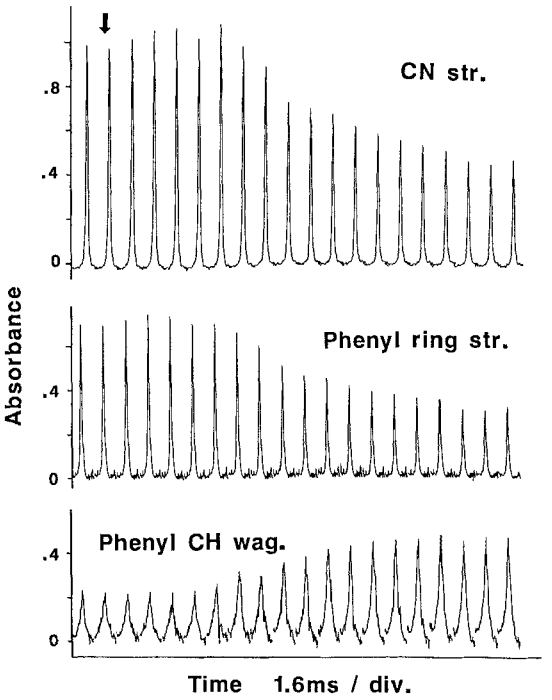

FIGURE 7 Time-dependent variations of the three major absorption bands during the homogeneous-to-homeotropic transition of 5PCH taken from the time-resolved parallel polarized absorption spectra ($A_{\parallel}$). The position of the DC field application is indicated by an arrow.

tensities of the C≡N absorption and the phenyl C—C absorption, both polarized parallel to the cyanophenyl *para*-axis, decrease at the same rate as the transition proceeds. This indicates that the cyanophenyl group reorients as a unit in response to the applied DC field. On the other hand, the phenyl C—H wagging band at 833 cm^{-1} increases its intensity in the transition region, in accord with the fact that its transition dipole moment is oriented perpendicular to the long molecular axis.

In the present study we have focused our attention to the rise-time dynamics of the homogeneous-to-homeotropic transition that has a response time of the order of milliseconds, but have not examined the decay process after the removal of the field. One practical difficulty was that the latter process has a much longer relaxation time (hundred of milliseconds) and our sub-millisecond instrument could not cover this range. However, we have observed in an independent 2D FT-IR TRS study[2] that the terminal pentyl chain of 5CB reorients faster than the cyanobiphenyl core (probably in the decay process from the homeotropic state to the homogeneous state). If such different time-dependent responses are proved to exist generally in nematic liquid crystals consisting of rigid and flexible segments, a completely new description of the field-induced transition of liquid crystals may be developed at the molecular segmental level. Obviously, we need further work to confirm this phenomenon for 5PCH and other nematic liquid crystals. Moreover, we anticipate that the 1D or 2D TRS experiment focused on the relaxation process may separate and identify hidden absorption peaks (such as the alkyl chain vibration band expected at the same position of the phenyl C—H wagging band) if in fact they have different response times in the relaxation process.

Finally, we discuss the effect of temperature on the reorientation rate. Shown in Figure 8 are the plots of the peak intensities of the C≡N stretching band and the phenyl C—C stretching band measured at 40 and 50°C. The reorientation rate increases as the temperature increases. That is, the midpoint of the transition shifts

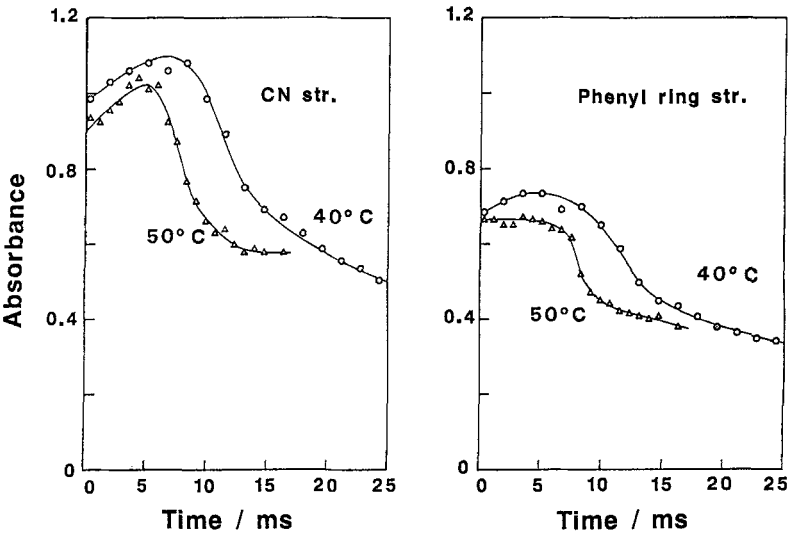

FIGURE 8 Time-dependent variation of the peak intensities of the C≡N stretching band (left) and the phenyl C—C stretching band (right) of 5PCH at 40 and 50°C.

from 12 ms at 40°C to 8 ms at 50°C. This change can be attributed to a decrease in the rotational viscosity at increased temperatures. A slight increase in the peak intensity in the induction region (which is more evident for the C≡N stretching band) is an artifact due to depolarization of the transmitted light. This effect, possibly arising from light scattering due to director fluctuations associated with certain pre-transition phenomenon, should cause larger influences in more intense absorption bands. It may be possible to eliminate or reduce this effect by using a thinner sample cell.

5. CONCLUSION

This paper has described the results of a time-resolved infrared study of the electric field-induced homogeneous-to-homeotropic transition in the nematic 5PCH liquid crystal. The average molecular orientation and its time-dependent variation during the transition are evaluated from static and dynamic polarized infrared measurements, respectively, using a rapid-scan FT-IR spectrometer. The homogeneous-to-homeotropic transition of 5PCH exhibits an induction period of several milliseconds and is completed in 10–20 ms. This relatively slow transition can be analyzed at the lowest time resolution level of our spectrometer (1.6 ms). With an available maximum resolution of 10 μs, we can analyze much faster transient phenomena occurring in the microsecond region. Examples of such μs-TRS measurements will be reported in subsequent papers for ferroelectric smectic liquid crystals.[12] The results obtained in this study demonstrate that FT-IR TRS, with the capability of obtaining simultaneous temporal and spectral resolution, can provide valuable new information concerning the elementary molecular processes underlying the time-dependent electro-optic phenomena exhibited by liquid crystals.

References

1. H. Toriumi, H. Sugisawa and H. Watanabe, *Jpn. J. Appl. Phys.*, **27**, L935 (1988).
2. V. G. Gregoriou, J. L. Chao, H. Toriumi, and R. A. Palmer, *Chem. Phys. Lett.*, **179**, 491 (1991).
3. R. E. Murphy, F. M. Cook, and H. Sakai, *J. Opt. Soc. Am.*, **65**, 600 (1975).
4. H. Sakai and R. E. Murphy, *Appl. Opt.*, **17**, 1342 (1978).
5. A. W. Mantz, *Appl. Spectrosc.*, **30**, 459 (1976); *Appl. Opt.*, **17**, 1347 (1978).
6. J. F. Durana and A. W. Mantz, *Fourier Transform Infrared Spectroscopy, Applications to Chemical Systems*, edited by J. R. Ferraro and L. J. Basile, Academic Press, New York (1979), vol. 2, p. 1.
7. P. R. Griffiths and J. A. de Haseth, *Fourier Transform Infrared Spectroscopy*, Wiley-Interscience, New York (1986), p. 387.
8. A. Hatta, *Mol. Cryst. Liq. Cryst.*, **74**, 195 (1981).
9. G. W. Gray and A. Mosley, *Mol. Cryst. Liq. Cryst.*, **35**, 71 (1976).
10. W. Maier and A. Saupe, *Z. Naturforsch., A.*, **14**, 882 (1959); **16**, 287 (1960).
11. D. J. Photinos, E. T. Samulski, and H. Toriumi, *J. Chem. Phys.*, **94**, 2758 (1991); *Mol. Cryst. Liq. Cryst.*, **204**, 161 (1991).
12. H. Sugisawa, H. Toriumi, H. Watanaba, K. Iwata, H. Hamaguchi, and I. Nishiyama, in preparation.